X-ray Investigation of Microstructure and Properties Evolution on Superalloy Inconel-718 derivative during Rapid Joule Heating and Severe Plastic Deformation In-situ

L. Kommel[1], R. Traksmaa[1], V. Mikli[2]

[1]*Department of Mechanical and Industrial Engineering, Tallinn University of Technology, Ehitajate tee 5, 12618 Tallinn, Estonia.*

[2]*Derpartment of Materials and Environmental Technology, Tallinn University of Technology, Ehitajate tee 5, 12618 Tallinn, Estonia.*

E-mail: lembit.kommel@taltech.ee.

ABSTRACT

The purpose of this study is to X-ray line-profile analysis of the effect of rapid Joule heating and severe plastic deformation in-situ on microstructure and properties evolution in polycrystalline austenitic Fe-balanced superalloy EP718E, which is Inconel 718 derivative. The microstructure of superalloy at different stages of processing was examined by X-ray diffraction, by scanning electron microscopy, and by energy dispersive spectrometry techniques. The mechanical properties evolution was studied by means of tension and high cycle fatigue testing's. The results of X-ray study show that the intensity, raw areas and net areas were step–by–step changed according to processing routines. Is shown that under shear stress the fcc-crystallites were deformed and the peaks parameters by 2-Theta scale changed partly.

Keywords: X-ray line-profile analysis, Inconel-718 derivative, electric upset forging, crystallites deformation, high cycle fatigue.

1. Introduction

In modern aircraft bypass turbofan engines [1] the most stressed parts, which define engine resource and lifetime extension, are the high pressure compressor (HPC) rotor blades. The rotor blades of HPC experience tension stress during rotor rotation at centrifugal forces, and torsion bending at the air flow. The blades are stressed by tensile-compression loads at vibration with different voltage levels. The amplitude and frequency of stresses varies in a wide range of voltages depending on the number of blades on the rotor stage and the number of blades on the stator stage as well as the rotor rotation frequency of turbojet engine [2, 3]. Uneven heating leads to cracks due to thermal stresses, which can develop into fatigue cracks [4]. In addition to the mechanical loading, the HPC blades operate in a corrosive air environment during long-time exposure at high temperatures [5, 6]. The temperature increases take place during supersonic flight as result of air braking and air compression in the compressor. The temperature on the last stages of the HPC blades increased up to 600-700 ºC. This necessitates the manufacture of the HPC

blades from polycrystalline NiFeCr-based superalloy Inconel 718 (IN718) [7] or its derivatives like EP718E [8]. These superalloys have small differences on chemical compositions and microstructure (see Tab. 1). IN718 is an age-hardenable austenitic Fe-balanced superalloy [9]. The mechanical strength of this material is largely dependent on the precipitation of a γ'-phase forming during thermomechanical treatment for producing optimum properties [10]. The microstructure of IN718, especially with regard to the effects of heat treatment, has been extensively studied and reported in [11]. The minor phase's evolution of IN718 takes place during long-time exposure at high temperatures and the principal phases γ', γ" and δ were coarsened. The literature has to be consulted for detailed discussions on the various phases developed by various heat treatments and other investigations of metallurgical processes [12-14]. An additional problem is associated with naval aviation. On aircraft carriers and on helicopter carriers, the turbo jet engines of the fighters and of the helicopters ingest salt from seawater. Salt leads to the destruction of superalloys by grain boundaries at intercrystallite erosion. By this the hydrogenated IN718 show ductility decreases (at tension) as well hydrogen embrittlement sensitivity of this alloy [15-16]. Thus, prolonged work in these conditions needs materials with specifically improved properties. Unfortunately, the influence of the rapid Joule heating by electric current with high density and severe plastic deformation (SPD) concurrently at different levels of heating rate and deformation degree have been studied in our own previous works [3, 17, 18] only. This technique for exploitation properties of superalloy IN718 and EP718E improve called as electric upset forging (EUF) process. For the deep study of these changes in material during thermo-mechanical processing and exploitation the powerful X-ray test technique [19-21] can be used. It is common knowledge that the peaks of X-ray intensities depend on material thickness, grain sizes, dislocation densities as well as porosity, both of which determine how X-rays penetrate, dissipate, absorb, and deflect. The anisotropic deformation during the EUF process can lead to the formation of anisotropic crystallites and consequently anisotropic X-ray peak broadening. The objective of the current study is to review by X-ray line-profile analysis at different stages of samples processing the effects of the rapid Joule heating and severe plastic deformation (SPD) concurrently (at different levels EUF processing and at followed die forging) on microstructure evolution and properties improve of material.

2. Experimental

Chemical composition of polycrystalline superalloy IN718 [7] and EP718E [8] (derivative of IN718, used in experiments), is presented in Table 1. As shown, the chemical content of superalloys has very small differences on Ni and Fe contents. The light elements (C, Si, Mn and B) are not presented in Table 1 for superalloy EP718E. The EP718E is an experimental alloy and its chemical composition is measured in four samples by (HR SEM - Gemini, LEO, Supra 35) SEM-EDS testing. The X-ray investigations were made by X-ray diffractometer D5005 Bruker AXS according to Database: ICDD PDF-4+2014 in middle part of cross-sections of EUF processed sample (Fig. 1, a, b). The X-ray patterns are presented without K-alpha2 lines and smoothed with Fourier filter. The peaks parameters are calculated after debugging. It has to be noted that before X-ray testing the cross-sections of samples were cut to identical measures. The microstructure evolution and precipitations content changes were studied across four stages of processing: I – initial condition of heat rolled rods, II – heat treated up to deformation starting temperature, III –

deformed up to 5-10% of strain, and IV – deformed up to 80 % of strain. Two zones of severe plastic deformation (SPD-I and SPD-II) by white dot lines are shown in Fig. 1, b. We propose to compare the two different technologies for HPC blades preforms manufacturing: by conventional technology and proposed technology that employ an electric upset forging (EUF) technique. This process, characterized by a rapid Joule heating and severe plastic deformation, is concurrently the workpiece part under upsetting that is heated up to a temperature at which deformation starts under corresponding axial compression stress. Preforms profiling was conducted on the EUF machine tool "Hasenclever-125/560". The initial samples have diameters of 12 mm and lengths of 85 mm. We propose for rods profiling a continuously consistent way [17] of EUF without admission on non-deformable length of the rod under fine die forging of the HPC blades (Fig. 1, a). For processing the radial electrodes (Fig. 1, a, 5 and 7, respectively) their length was increased to two length of rod workpiece before processing and the punch has a lower diameter then the workpiece. The EUF parameters were the following: effective deformation load F_d = 62 kN, electric current I = 4300 A, current density i = 38 A/mm^2, heating rate Δt = 130 ºC·s^{-1}, heating time up to deformation starting τ = 7 s, deformation starting temperature t_1 = 910±5 ºC, maximal temperature inside of the sample deformed part was increased to t_2 = 1020±5 ºC. During EUF the diameter of samples was increased from 12 mm to ~30 mm (Fig. 1, b) and at follows the EUF processed preforms were die forged on press without (or with) additional furnace heating. The macrostructure of EUF processed preform under die forging of HPC blade in longitudinal section is shown in Fig. 1, b. This technique also includes high accuracy die forging under isothermal conditions on a hydraulic press immediately after profiling the round sample and stamping with high accuracy on an electric stator press followed trimming of flash in trimmer die by the crank press. At follows the 6 forgings and for comparison 6 forgings produced by conventional technology were heat treated at 1000 ºC for 2 h and cooled in oil. Then the 1-st aging was made at a temperature of 780 ºC for 5 h with air cooling; 2-nd aging was made at 650 ºC for 16 h followed air cooling. According to these techniques, after mechanical cutting of the dovetail root-blade, the HPC blades were cold rolled to measures and the surface of each blade was polished to finish.

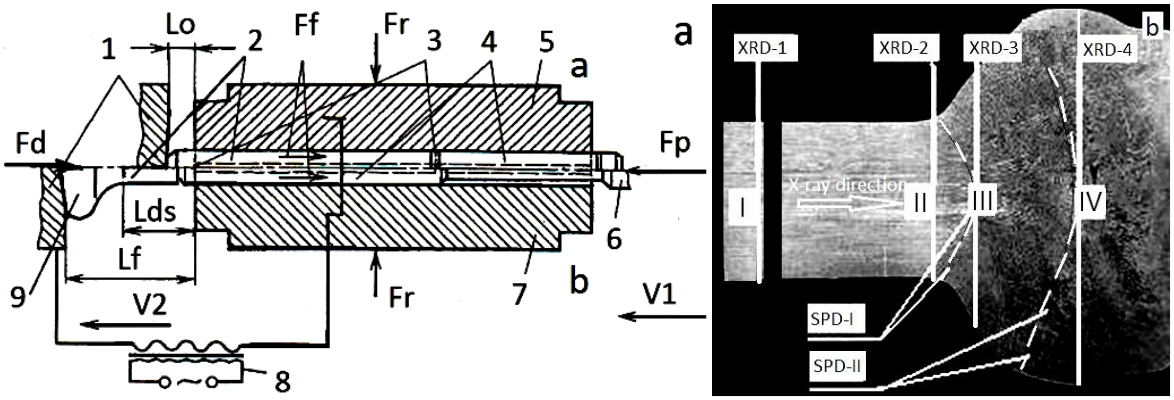

Fig. 1. Scheme of a continuously consistent method [17, 18] for HPC blades preform manufacturing according to proposed EUF process. Designations (in Fig. 1, a): a - initial stage (hight) of EUF process; b-end stage (lower) of EUF process; (c) L_o – initial distance between electrodes, L_{ds} – distance of deformation starting at heating, L_f – final distance between electrodes; (d) F_f – friction force, F_r – radial loding force for pressure of radial electrodes to sample, F_p – pressure load, F_d – deformation load; (e) V_1 – punch rate of

the sample moving, V_2 - removal rate of the end electrode; 1- end electrode, 2- samples, 3 – conical end part of sample, 4 – cilindrical rods at starting measures, 5 – upper radial electrode, 6 – punch, 7 – lower radial electrode, 8 – electrical transformer, 9 – upsetted preform under HPC blade die forging. The XRD testing zones in cross-section of preform as well as X-ray direction and SPD-I and SPD-II regions, and microstructure investigation zones (I-IV) in longitudinal section of preform are indicated in Fig. 1, b.

Table 1. Chemical compositions of superalloys IN718 [7] and EP718E (SEM-EDS).

Material	Ni	Fe	Al	Ti	Cr	Mo	W	Nb	Si	C	B	Mn	%
IN718	53.38	17.01	0.6	1.08	18.9	3.15	0.1	5.48	0.04	0.04	0.01	0.04	99.83
EP718E	42.84	27.66	0.8	2.42	14.84	4.72	5.14	0.96	-	-	-	-	99.4

Material tension strength was investigated by examining mini samples (at least 3-4 samples for one test region) which were cut off from initial material and all three stages of EUF processing as well as from HPC blade dovetail root-blade. The mini samples for tension testing have dimensions of 0.5x2x5 mm on test part. The HCF tests of finished blades of 6 pieces for two manufacture technologies were performed on an electrodynamics shaker at ambient temperature with frequency rate of $F_{1,0}$ = 1110 - 1180 Hz. The high cycle fatigue (HCF) was studied on four test intervals at loads with corresponding stresses of 260-360 MPa, 360-440 MPa, and 360-440 MPa (for blades produced by conventional technologies, for comparison) and 440-600 MPa (for HPC blades produced by proposed technology), respectively. During the HCF test the level of stress was set with the step-by-step load increase and the endurance data for EP-718E was received. The tests were carried out for different values of δ_{-1}, which are altered in stages. If any voltage value had achieved N = $2x10^7$ cycles without failure, the δ_{-1} was increased to 40 MPa and the test was repeated with the new voltage up to N = 2 $x10^7$ cycles. If failure occurred, then the load was reduced by δ_{-1} = 40 MPa for other HPC blades. The HCF tests was limited by the maximum stress level of δ_{-1} = 600 MPa.

Results and Discussion

3.1. X-ray investigation

The X-ray investigation of line-profile analysis of the 5 peaks (Fig. 2, a) in interval from 40º to 100º of 2-Theta were investigated. The parameters calculated and results are presented in Fig. 3 diagrams. Dependence on processing stages the X-ray intensity was increased mainly at all steps of processing (Fig. 2, b-f and Fig. 3). The intensity was decreased during Joule heating as the grain boundaries (GB) structure was changed. The parameters of peaks like width (or half-width) and the shape of the geometry of the surface were calculated (Fig. 3, b). They depend on the first try - it is a plane, or a convex, or concave, or smooth. The material grain size and the crystalline degree has influenced on the X-ray intensity also. For example, from the large single crystal the thinnest peak can be formed, increasingly finer crystal diffraction broader peak until the transition to the amorphous state. The peak is going to a very wide back-cloths, recovery of material density how deep X-ray beam in the material penetrates, peak geometry again depends on effect of the processing modes and parameters. The intrinsic tension in the deformed material is

available. Part of the crystal planes either compressed or stretched out - their levels by diffraction radiation intensity maximum shifts the 2-Theta scale slightly and gives results in wider alliances of peak.

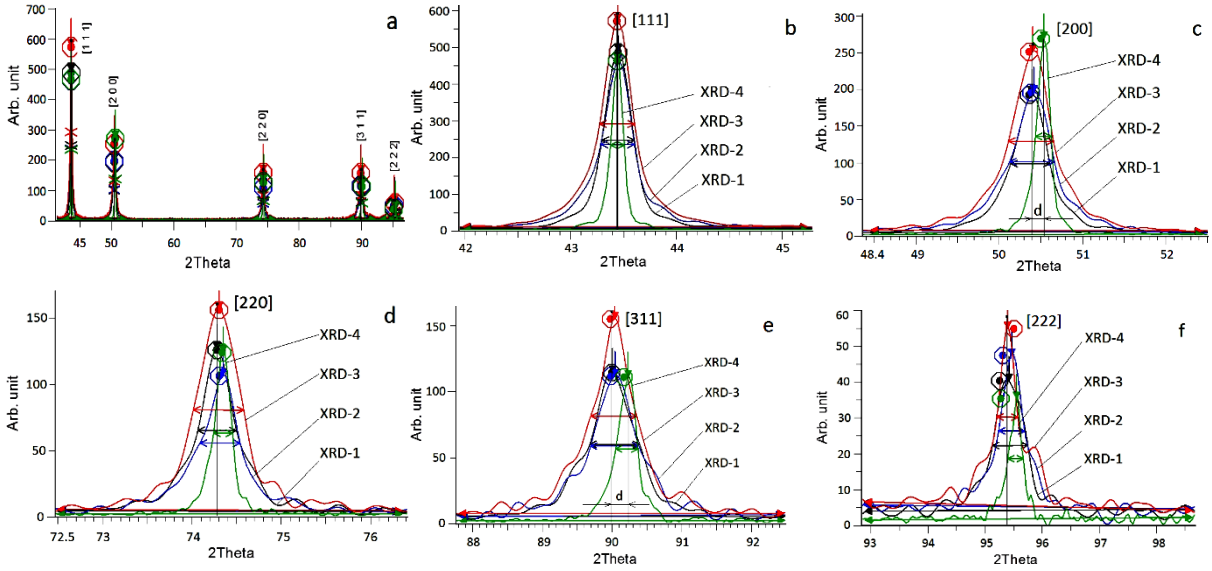

Fig. 2. The measured X-ray diffractogram (a) and fife peaks (b-f) for [111], [200], [220], [311] difractograms of initial (XRD-1), Joule heated (XRD-2), Joule heated and deformed about 5% of strain (XRD-3), and Joule heated and deformed about 80% (XRD-4), respectively.

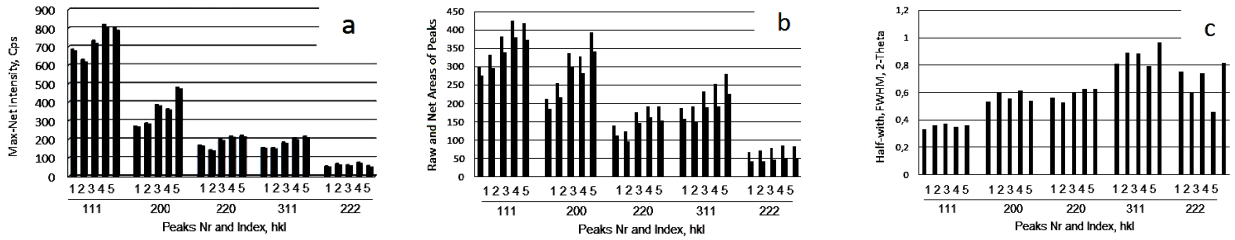

Fig. 3. X-ray peaks calculated parametes: a - Maximal and Net intensity of peaks, b - Raw and Net areas of peaks, c - Half-width, FWHM, of 2 - Theta.

The distances (d) on planes [200] and [311] were changed (Fig. 2, c and e) as the crystallites were deformed under shear stress. To protect from the continuous oxidation of the grain boundaries is necessary to eliminate the defects of the microstructure, which limits the diffusion of oxygen into the material.The microstructural analyzes show that the microstructure heterogeneity of superalloy is due to differences in the deformation. In doing so, the material heats up at different rates, and the heating rate depends mainly on current density. As a result, the metal in deformed part of sample has different temperatures at the end of EUF process. At such heterogeneity of temperatures and intrinsic stresses, compression stress in central part and tension stresses on surface, leads to forming different microstructures and mechanical properties.

3.2. Microstructural investigations

The hot rolled rods' initial microstructure (Fig. 4, a) before EUF processing shows many small bores on boundaries confluences of three grains as metallurgical defects. The maximal sizes of bores was about 200-300 nm (Fig. 4, b). The eliminating of microstructure defects like ultrafine size bores at the confluence of GB and GB improve is the main requirement for proposed technology. These defects cause the metal

intergranular erosion by hydrogen of HPC blades mainly in the naval aviation [15, 16]. At follows we show also by high cycle fatigue (HCF) testing, that during EUF processing the elimination of nanoporous increases the life extension of HPC blades. During Joule heating concurrently with small (to ~5%) degree of deformation the grain size was increased from ~10 μm to ~20 μm or about two times (Fig. 5, b) on second stage of processing. Such evolution of microstructure during processing is shown in Fig. 5. The figure shows grain size increasing during rapid heating with very small deformation as evident in Fig. 5, b. At increased degree of von Mises strain during severe plastic deformation (see Fig. 1, SPD-II) the grain size was significantly decreased to some micrometers in size (Fig. 5, c) at strain of 80 %. The slip bands were formed inside of grains and the dislocation density increased, respectively. The changes in the chemical state of phases in initial and three sections after the high-speed electric-heating and severe plastic deformation of workpiece were investigated by electron diffraction technique (Fig.6). In our study, we consider the billet of superalloy as a closed system wherein the amount of chemical elements in material was constant during processing (see Tab.1. EP718E). The results achieved by SEM-EDS investigation are presented in SEM scans in Fig. 6 and in Table. 2, respectively. The microstructure also contains Cr-Mo-W-rich compound, and Ti-Nb-C and T-C carbides. The results of SEM-EDS investigation show that precipitation phases' content is about 1.9 wt.% in alloy. The changes in chemical composition of GB was tested by leaching in HCl acid. The comparison of GB leaching of initial (is presented in Fig. 4, c, d) and by EUF processed material (is presented in Fig. 4, e, f), respectively. It can be seen that the material GB after proposed EUF process with 80 % of deformation, is stable to chemical leaching as well as to sea water influence on GB erozion during exploitation in naval aviation.

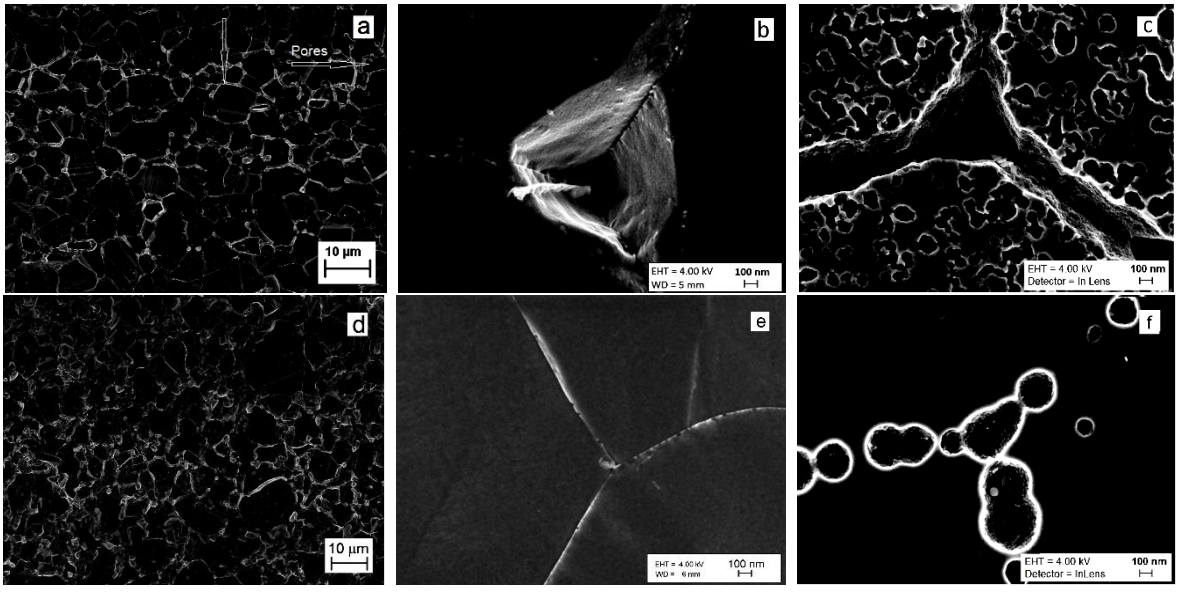

Fig. 4. The SEM scans of the initial EP718E sample (a), the metallurgical defects, pores at the confluence of three grains (b), triple GB erosion after chemical etching (c) and after EUF processing (d, e) and followed chemical etching with HCl (f).

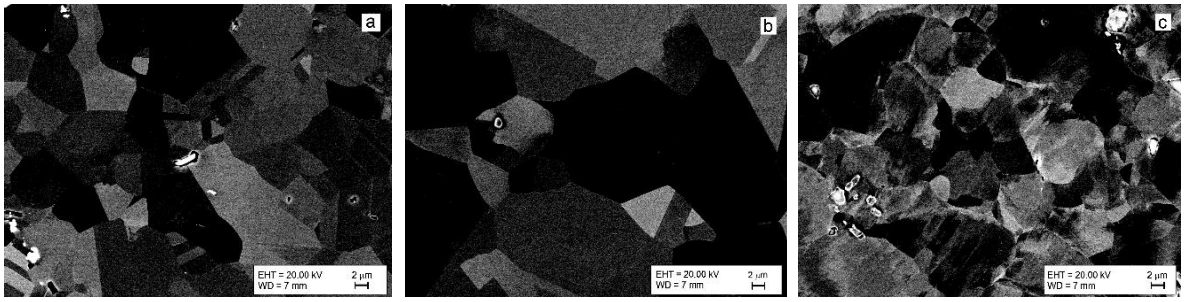

Fig. 5. The SEM scans of the sample after rapid Joule heating (a), deformation to 5% (b) and deformation up to 80%, respectively.

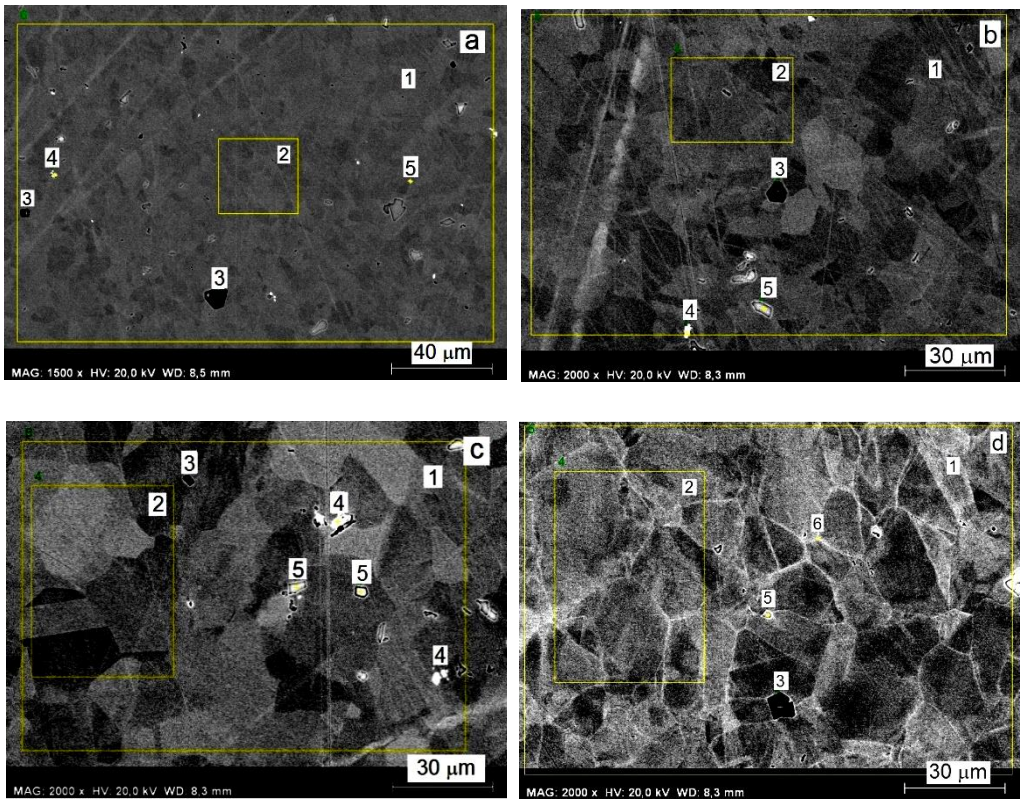

Fig. 6. EDS-SEM investigation of chemical compositions in samples: a – initial, b – rapidly Joule heated, c – heated and deformed to ~5% of strain and d – heated and deformed to 80% of strain. Definitions (in Tab 2): 1 – all surface include phases, 2 – surface with no inclusions, 3 –Ti-rich areas (black), 4 –Ti-Nb rich area (light-gray), 5 –Mo-Nb-W rich area (white), and 6 – newly formed GB area with Ni-rich chemical composition (in Fig. 6, d).

Table 2. Mean chemical composition of the alloy IN718 derivative and its phases.

Phases Nr in Fig. 6.	Ni	Fe	Cr	W	Mo	Ti	Nb	Al	Wt. %
1. EP718E	42.84	27.66	14.84	5.14	4.72	2.42	0.96	0.81	99.4
2. No precipitations	42.79	27.22	14.36	5.07	4.52	1.96	0.78	0.8	97.5
3. Ti-rich	1.57	1.17	0.89	-	-	88.78	3.14	-	95.6
4. Ti-Nb-rich	1.55	1.15	0.98	6.93	-	35.98	50.6	-	97.2
5. W-Mo-rich	16.01	14.5	12.4	13.3	28.1	2.67	7.15	-	-
6. GB	45.32	26.63	14.99	5.42	4.94	2.83	0.78	0.88	101.78

3.3. Tension and HCF testing's

Results show that the initial material (Sample N1, Conventional) shows highest value at tension revealed to 1266 MPa but the minimal elongation of 22 % to failure (Fig. 7, a). During rapid Joule heating (Sample N2) with heating rate of 110 °C/s the tensile stress was decreased to 1015 MPa and elongation increased to 55 %. During SPD starting at 5 % (Sample N3) the heated material tensile stress increased to 1064 MPa but elongation decreased to 48 %. By increasing SPD to ~80 % (Sample N4) the elongation was increased to 56 %. Compared to initial material the Young modulus was lowered during rapid heating (see initial loops of curves N2, N3 and N4). During furnace heating and die forging decreases the tensile stress to 957 MPa, but the Young modulus (see Fig. 7, curves N5 and N6) increased significantly. Results shows that Young modulus of materials was lowered during EUF, suggesting that during rapid heating decreases the interatomic forces. The Young modulus increased at followed die forging of preforms. High cycle fatigue (HCF) and high-frequency strength (HFS) are important quality properties of HPC blade material as they determines the resource of the turbo-jet engine.

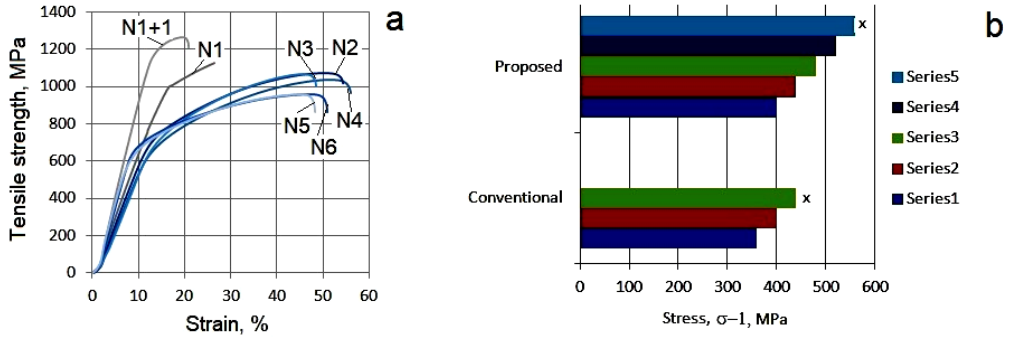

Fig. 7. Tension stress (MPa) at corresponding strain (%) curves (a) and endurance data at HCF cyclic tension-compression stress (δ_{-1}) values (b) dependence on processing technologies (Conventional - Proposed) at corresponding test series of EP718E superalloy. By asterisks (in b) is shown fracture at corresponding stress (δ_{-1}) values and at cycle's number lower then $2x10^7$.

Results of HCF testing of blades produced by conventional technology show that the maximal fatigue strength δ_{-1} = 400 MPa was obtained at second tests series (Fig. 7, b). By increased stress up to δ_{-1} = 440 MPa the conventional blades were fractured at different cycles number and mainly on distance of 2-3 mm from root blade. The microstructure in this part of HPC blade was coarse grained as in initial material. It was found that the application of electrical upsetting for production of preforms under precise isothermal forging of blades increases the fatigue strength to δ_{-1} = 520 MPa or about 30 % compared to conventional technology produced by hot extrusion followed hot rolling of preforms of HPC blade. As you can see during HCF testing the stress was lowered about two times then at tension testing. The HPC blades produced by proposed technology have identical fine grained microstructure in all parts of blade. By this, according to technical requirements [18] the HPC blades had to withstand fatigue strength of δ_{-1} = 320 MPa at $2•10^7$ cycles. So that the HPC blades which were produced by proposed technology has increased fatigue stress of δ_{-1} = 520 or ~62 % higher with compare to technical requirements, or ~30 % higher compared to conventional technology. In this study the cycle's number to failure during HCF increased four times.

3.4. X-ray analize for life extension improvement mechanisms study

This mechanism include: a) highest heating rate on GB as the electrical resistance is higher on GB with compare to single crystal (according to Joule-Lenz law); b) highest temperature on GB, lower resistance to deformation (at simple shear stress) as material is softer; high temperature on GB influence the interdiffusion of chemical elements between GB and single crystal; c) solid-solid phase transformations and new grains forming via connection to neighboring grains during Joule heating and at small (~5 %) compression deformation; d) X-ray intensity (XRD-2) was decreased as the grain size was increased during rapid Joule heating with very small deformation (see Fig. 3, a). Simultaneously, at followed severe plastic deformation (see Fig. 1, b, region SPD-II) at simple shear stresses the grains elongation take place in the direction of metal flow and defects on GB confluence three neighboring grains are compressed to zero. Extension of the peaks' half-width (Fig. 3, c) indicates that in the SPD-II zone (Fig. 1, b) under shear stress the smaller crystallites are formed (Fig. 5, c). In this zone is also the grain boundaries enriched by nickel of up to 45.3 wt.% (see Tab. 2 and Fig. 6, a). There was also a slight increase in W and Mo, but the Nb and Fe content was reduced. It is well known that the stress gradient heterogeneity or microstructural heterogeneity if UFG metals can also cause peak broadening [21]. The microstructural heterogeneity formed during EUF can also cause peak broadening (Fig. 3, b). The peak asymmetry will be caused by long-range internal stresses as well as chemical heterogeneity change. The anisotropic deformation during the EUF process can lead to the formation of anisotropic crystallites and, consequently, anisotropic peak broadening. Mechanical properties, high temperature strength and high cyclic fatigue of superalloy depends on inclusions, nanorange defects and non-wetting of grain boundaries and also the chemical content of grain boundaries changes (Ni content on GB was increased) and phase's state stabilization take place [22]. This study also shows that the GB were at diffusion enriched by Ni and defects on confluence of three grains were eliminated. Such process is described in [23, 24]. The tensile strength as well as Young modulus were lightly decreased but elongation was increased up to three times during EUF-treatment. As you can see (Fig. 7, a) the tensile stress was up to two times higher then the stress which was used during HCF testing (Fig. 7, b). As result, the HCF strength was increased from 300 to 560 MPa and life extension for $2 \cdot 10^7$ cycles was increased up to 4 times (see Fig. 7, b). During HCF testing the load was step-by-step increased so that the stress was increased by 40 MPa after testing at fully $2 \cdot 10^7$ cycles. Results revealed that the HPC blades with EUF-treatment of preforms exibited longer HCF life then those of the untreated blades. The improvement in HCF life is mainly attributed to the induced by fast Joule heating on GB to higher temperature then in crystallites. The chemical composition of GB was changed [25] as the Ni-content increased on GB (see Tab. 2). The mechanism of oxigen-induced intergranular fracture reduce the GB energy [26-28] in such way that the crack growth path becomes intergranular along rapid diffusion paths.

Conclusions

Results revealed that the life extension and fatigue improvement mechanisms include: a) microstructural defects on GB liquidating; b) Ni content on GB increasing; c) grains refinement at shear stress at final stage of processing; d) resistivity to chemical leaching increasing. The HPC blades, produced with EUF

treatment of preforms under stamping, exhibited longer HCF life than those of the produced by conventional technology. The increase of blades exploitation properties were received in the results of GB defects and the defects on confluence of three grains were eliminated at rapid Joule heating and shear stress of deformation concurrently. This work concludes: it is sufficient to explain the existence of electric current and shear deformation activated grain boundary motion and chemical content change on grain boundaries. The effect of the EUF is to increase the HCF stress/strength and life extension of HPC blades processed by proposed technology from superalloy EP718E has been proven and discussed by X-ray line-profile analysis of microstructure at different stages of HPC blades manufacturing in industry.

Acknowledgements: The research was supported by Estonian Ministry of Education and Research by Project IUT1929. This work was part of a bilateral project between the Bulgarian Academy of Sciences and Estonian Academy of Science, Tallinn University of Technology (TalTech) by projects TAR16016 and IUT-T4.

References

[1] Information on http://www.npo-saturn.ru/ (Engines for military aircrafts UAS, AL-31F, 117S, AL-55).

[2] D.G.L. Prakash, M.J. Walsh, D. Maclachlan, A.M. Korsunsky, Crack growth micro-mechanisms in the IN718 alloy under the combined influence of fatigue, creep and oxidation. Int. J. Fatigue 31 (2009) 1966-1977.

[3] L. Kommel, Microstructure and properties characterization of polycrystalline Ni-Fe-Cr-based superalloy EP-718E after electric upsetting. TTP, Key Eng. Mater. 721 (2017) 467-472.

[4] W. Maktouf, K. Sai, An investigation of premature fatigue failures of gas turbine. Eng. Failure Analysis 45 (2015) 89-101.

[5] M.C. Rezende, L.S. Araújo, S.B. Gabriel, J. Dille, L.H. de Almeida, Oxidation assisted intergranular cracking under loading at dynamic strain aging temperatures in Inconel 718 superalloy. J. Alloys and Compounds, 643 (2015) S256-S259.

[6] D. Srinivasan, Effect of long-time exposure on the evolution of minor phases in Alloy 718. Mater. Sci. Eng. A364, 1-2 (2003) 27-34.

[7] Information on http://www.specialmetals.com.

[8] Information on http://www.npo-saturn.ru/ (Expertise, Products, Services- Sukhoi-27).

[9] J. Calvo, S. Shu, J.M. Cabrera, Characterization of precipitation kinetics of Inconel 718 superalloy by the stress relaxation technique. TTP, Mater. Sci. Forum 706-709 (2012) 2393-2399.

[10] H. Zhang, C. Li, Y. Liu, Q. Guo, H. Li, Precipi-tation behavior during high-temperature isothermal compressive deformation of Inconel 718 alloy. Mater. Sci. Eng. A677 (2016) 515-521.

[11] G.A. Rao, M. Srinivas, D.S. Sarma, Effect of thermomechanical working on the microstructure and mechanical properties of hot isostatically pressed superalloy Inconel 718. Mater. Sci. Eng. A383 (2004) 201-212.

[12] L. Chang, W. Sun, Y. Cui, R. Yang, Precipita-tion of hot-isostatic-pressed powder metallurgy super-alloy Inconel 718 free of prior particle boundaries. Mater. Sci. Eng. A 682 (2017) 341-344.

[13] L. Xiao, D.L. Chen, M.C. Chaturvedi, Cyclic deformation mechanisms of precipitation-hardened Inconel 718 superalloy. Mater. Sci. Eng. A483-484 (2008) 369-372.
[14] M. Zouari, N. Bozzolo, R.E. Loge, Mean field modeling of dynamic and post-dynamic recrystallization during hot deformation of Inconel 718 in the ab-sence of δ phase. Mater. Sci. Eng. A655 (2016) 408-424.
[15] T.S.A. Rosa, A.F. Ribeiro, L.H. de Almeida, D.S. dos Santos, Effect of the microstructure on the hydrogen diffusivity in Ni-based superalloy 718. TTP, Def. Dif. Forum 297-301 (2010) 733-738.
[16] L. Liu, C. Zhai, G. Lu, W. Ding, A. Hirose, K. F. Kobayashi, Study of the effect of δ phase on hydrogen embrittlement of Inconel 718 by notch tensile tests. Corrosion Science 47 (2005) 355-367.
[17] L.A. Kommel, G.P. Teterin, A method for manufacturing one locking blade of the compressor of the turbojet. Patent SU Nr. 1552458 A1 (1988) of USSR (in Russian).
[18] L.A. Kommel, G.P. Teterin, Electric upset forging of preforms for short blade stamping of turbojet compressor. Forging and Stamping Production, 10 (1998) 18-22 (in Russian).
[19] J. Tiley, G.B. Viswanathan, J.Y. Hwang, A. Shiveley, R. Banerjee, Evaluation of gamma prime volume fractions and lattice misfits in a nickel base superalloy using the external standard X-ray diffraction method. Mater. Sci. Eng. A 528 (2010) 32-36.
[20] M. Fisk, J. Andersson, R. du Rietz, S. Haas, S. Hall, Precipitate evolution in the early stages of ageing in Inconel 718 investigated using small-angle x-ray scattering. Mater. Sci. Eng. A 612 (2014) 202-207.
[21] T. Ungár, E. Schafler, J. Gubicza, Microstructure of bulk nanomaterials determined by X-ray line-profile analysis. Bulk Nanostructured Materials. Edited by M.J. Zehetbauer and Y.T. Zhu, Copyright 2009 WILEY-VCH Verlag GmbH & Co. KGaA, Weinheim.
[22] Y.C. Lin, F-Q. Nong, X-M. Chen, D-D. Chen, M-S. Chen, Microstructural evolution and constitutive models to predict hot deformation behaviors of a nickel-based superalloy. Vacuum 137 (2017) 104-114.
[23] Z. Chen, M. Hörnqvist-Colliander, G. Sundell, R.L. Peng, J. Zhou, S. Johansson, J. Moverare, Nano-scale characterization of white layer in broached Inconel 718. Mater. Sci. Eng. A 684 (2017) 373–384.
[24] V.A. Popovich, E.V. Borisov, A.A. Popovich, V.Sh. Sufiiarov, D.V.Masaylo, L. Alzina, Functionally graded Inconel 718 processed by additive manufacturing: Crystallographic texture, anisotropy of microstructure and mechanical properties. Mater. Design 114 (2017) 441–449.
[25] A.B. Straumal, B.S. Bokstein, A.L. Petelin, B.B. Straumal, B. Baretzky, A.O. Rodin, A.N. Nekrasov, Apparently complete grain boundary wetting in Cu-In alloys. J. Mater. Sci. 47 (2012) 8336-8343.
[26] E. Andrieu, R. Molins, H. Ghonem, A. Pineau, Intergranular crack tip oxidation mechanism in a nickel-based superalloy. Mater. Sci. Eng. A154 (1992) 21–28.
[27] D.G.L. Prakash, M.J. Walsh, D. Maclachlan, A.M. Korsunsky, Crack growth micro-mechanisms in the IN718 alloy under the combined influence of fa-tigue, creep and oxidation. Int. J. Fract. 31 (2009) 1966-1977.
[28] P.M. Ruben, P-L. Thierry, C. Bathias, P.C. Paris, Very high cycle fatigue of a high strength steel under sea water corrosion: A strong corrosion and mechanical damage coupling. Int. J. Fatig. 74 (2015) 156–165.